Article

Electrochemical Investigation of Photooxidation Processes Promoted by Sulfo-polyoxometalates: Coupling of Photochemical and Electrochemical Processes into an Effective Catalytic Cycle

Thomas Rther, Victoria M. Hultgren, Brian P. Timko, Alan M. Bond, William R. Jackson, and Anthony G. Wedd

J. Am. Chem. Soc., **2003**, 125 (33), 10133-10143• DOI: 10.1021/ja029348f • Publication Date (Web): 24 July 2003

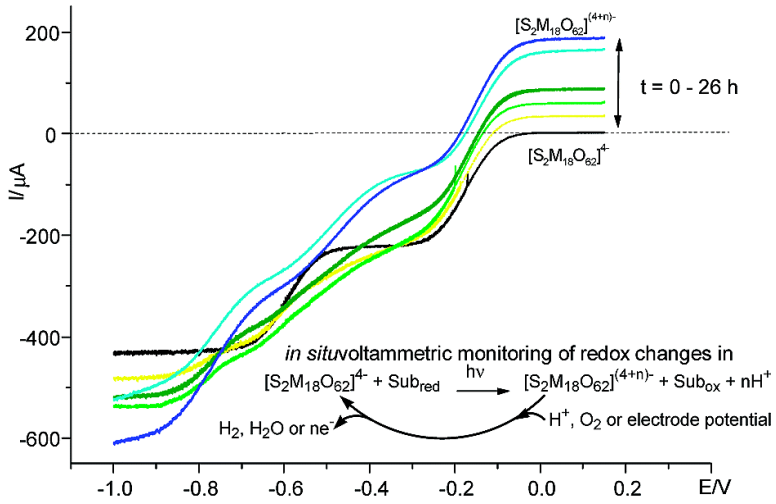

More About This Article

Additional resources and features associated with this article are available within the HTML version:

- Supporting Information
- Links to the 12 articles that cite this article, as of the time of this article download
- Access to high resolution figures
- Links to articles and content related to this article
- Copyright permission to reproduce figures and/or text from this article

View the Full Text HTML

J|A|C|S
ARTICLES
Published on Web 07/24/2003

Electrochemical Investigation of Photooxidation Processes Promoted by Sulfo-polyoxometalates: Coupling of Photochemical and Electrochemical Processes into an Effective Catalytic Cycle

Thomas Rüther,*,†,⊥ Victoria M. Hultgren,‡ Brian P. Timko,‡ Alan M. Bond,*,‡ William R. Jackson,† and Anthony G. Wedd§

Contribution from the Centre for Green Chemistry, Monash University, Box 23, Melbourne, Victoria 3800, Australia, Monash University, Box 23, Melbourne, Victoria 3800, Australia, and University of Melbourne, Parkville, Victoria 3010, Australia

Received November 14, 2002; E-mail: A.Bond@sci.monash.edu.au

Abstract: Oxidative photocurrents measured upon irradiation by a 7-W visible light (wavelength 312−700 nm) demonstrated that the sulfo-polyoxometalate anion clusters $[S_2W_{18}O_{62}]^{4-}$ (**1a**), $[S_2Mo_{18}O_{62}]^{4-}$ (**1b**), and $[SMo_{12}O_{40}]^{2-}$ (**2**) may be activated photochemically to oxidize the organic substrates benzyl alcohol, ethanol, and (−)-menthol. In the case of catalytic photooxidation of benzyl alcohol to benzaldehyde in the presence of **1a**, quantitative electrochemical methods have identified pathways for the oxidation of reduced forms of **1** generated during the catalysis. More generally, the oxidation pathways $P^{(n+2)-} + 2H^+ \leftrightarrows P^{n-} + H_2$ and $2P^{(n+2)-} + O_2 + 4H^+ \leftrightarrows 2P^{n-} + 2H_2O$ have been evaluated by monitoring acidified acetonitrile solutions of the 2e$^-$-reduced clusters by rotating disk electrode voltammetry under anaerobic and aerobic conditions, respectively. Neither of the reduced forms **1b**(2e$^-$) nor **2**(2e$^-$) reacted under these conditions. In contrast, **1a**(2e$^-$) was oxidized via both pathways, consistent with its more negative redox potential, with the rate of oxidation by air-oxygen being significantly faster than that by H^+. The present work demonstrated that the crucial step necessary to oxidize reduced catalyst in photocatalytic reactions involving the anions studied may be achieved or accelerated by application of an external potential more positive than the first redox potential of the polyoxometalate anion. Voltammetric analysis revealed that this in situ electrolytic regeneration of the reduced catalyst is an option that leads to a viable photoelectrocatalytic pathway, even when the H^+ and O_2 pathways are not available.

Introduction

In recent years, catalytic oxidation processes based on polyoxometalate redox chemistry have received considerable attention as environmentally and economically viable alternatives to classical stoichiometric methods, which use powerful oxidants such as chromate, permanganate, lead dioxide, nitric acid, and hypochlorite.[1] Apart from their ready availability and their low toxicity, these cluster anions have the attraction of being less prone to redox degradation than catalysts containing organic ligands.

Liquid-phase catalytic oxidation involving polyoxometalate anions is being addressed currently by four principal lines of research. Several groups have investigated H_2O_2 as an oxidant (Ventruello/Ishii chemistry).[1e,g,2] The second approach has employed mixed-addenda heteropolyanions such as $[PV_nMo_{12-n}O_{40}]^{(3+n)-}$ in electron-transfer redox-type oxidations.[1a,g,3] A third category has used a lacunary or unsaturated Keggin heteropolyanion, $[XM_{11}O_{39}]^{q-}$, to bind a transition metal cation,

† Centre for Green Chemistry.
‡ Monash University.
§ University of Melbourne.
⊥ Present address: IDT Australia Ltd., 45 Wadhurst Drive, Boronia, VIC 3155, Australia. Fax: +61 3 9837 6446.

(1) (a) Pope, M. T., Müller, A., Eds. *Polyoxometallate Chemistry*, Kluver Academic Publishers: Dordrecht, The Netherlands, 2001. (b) Pope, M. T., Müller, A., Eds. *Polyoxometallates: From Platonic Solids to Anti-retroviral Activity*; Kluver Academic Publishers: Dordrecht, The Netherlands, 1994. (c) Sheldon, R. A., vanBekkum, H., Eds. *Fine Chemicals Through Heterogeneous Catalysis*; Wiley-VCH: Weinheim, 2001. (d) Kozhevnikov, I. V. *Russ. Chem. Rev.* **1993**, *62*, 473. (e) Sanderson, W. R. *Pure Appl. Chem.* **2000**, *72*, 1289. (f) Hill, C. L., Guest Editor. *Chem. Rev.* **1998**, *98*, 1. (g) Hill, C. L.; Prosser-McCartha, C. M. *Coord. Chem. Rev.* **1995**, *143*, 407. (h) Pope, M. T.; Müller, A. *Angew. Chem., Int. Ed. Engl.* **1991**, *30*, 34. (i) Papaconstantinou, E. *Chem. Soc. Rev.* **1989**, *18*, 1. (j) Polyoxometalates in Catalysis. Hill, C. L., Ed. *J. Mol. Catal. A* **1996**, *114*, 1−371. (k) Sheldon, R. A.; Kochi, J. K. *Metal-Catalysed Oxidations of Organic Compounds*; Academic Press: New York, 1981.

(2) (a) Ishii, Y., Ogawa, M., Eds. *Hydrogen Peroxide Oxidation Catalyzed by Heteropolyacids Combined with Cetylpyridinium Chloride*; MY: Tokyo 1990; Vol. 3, pp 121−145. (b) Venturello, C.; D'Aloisio, R. *J. Org. Chem.* **1988**, *53*, 1553. (c) Venturello, C.; D'Aloisio, R.; Bart, J. C. J.; Ricci, M. *J. Mol. Catal.* **1985**, *32*, 107. (d) Ishii, Y.; Tanaka, H.; Nishiyama, Y. *Chem. Lett.* **1994**, 1. (e) Tsubakino, T.; Nishiyama, Y.; Ishii, Y. *J. Org. Chem.* **1993**, *58*, 671. (f) Sakata, Y.; Katayama, Y.; Ishii, Y. *Chem. Lett.* **1992**, 671. (g) Ogushi, T.; Sakata, Y.; Takeuchi, N.; Kaneda, K.; Ishii, Y.; Ogawa, M. *Chem. Lett.* **1989**, 2053. (h) Ishii, Y.; Yamawaki, K.; Ura, T.; Yamada, H.; Yoshida, T.; Ogawa, M. *J. Org. Chem.* **1988**, *53*, 3587. (i) Shimizu, M.; Orita, H.; Hayakawa, T.; Takehira, K. *Tetrahedron Lett.* **1989**, *30*, 471. (j) Schwelger, M.; Floor, M.; van Bekkum, H. *Tetrahedron Lett.* **1988**, *29*, 823.

(3) (a) Kozhevnikov, I. V. *Chem. Rev.* **1998**, *98*, 171. (b) Kozhevnikov, I. V.; Matveev, K. I. *Russ. Chem. Rev.* **1982**, *51*, 1075. (c) Misono, M. *J. Chem. Soc., Chem. Commun.* **2001**, 1141.

yielding a metal-substituted heteropolyoxometalate catalyst.[1g,4] The fourth type focuses on photooxidation promoted by polyoxometalate anions.[1i,5]

Irradiation of specific clusters with visible or near-ultraviolet light can promote a range of oxidation reactions that are thermodynamically or kinetically unfavorable in the dark. Key factors for the establishment of effective catalytic processes include identification of the active species and efficient catalyst regeneration and recovery. Peroxo complexes[2c,e,6] and intact polyoxometalates[7] have been identified as the active species in the H_2O_2 systems. Excited states of intact polyoxometalate anions operate in the photocatalytic systems.[1i,5] Oxidation of the reduced catalyst is an important step in photocatalysis and has been investigated to a limited degree only.[1i,f,5e,8] These studies employed UV−vis, NMR, ESR, IR, gas chromatography, and labeling techniques to show that (i) the catalytic cycle can be closed at the expense of molecular oxygen or hydrogen ions and (ii) the ease of oxidation (regeneration of catalyst) varies considerably between different cluster anions.

The essential reactions for a photocatalytic pathway are summarized in formal eqs 1−6, which contain the simplification of an overall two-electron oxidation of general substrate SH_2 by the polyoxometalate anion P^{n-}.

$$P^{n-} + SH_2 \overset{k_{EDA}}{\rightleftharpoons} P^{n-}\cdots SH_2 \quad \text{(EDA complex formation)} \quad (1)$$

$$P^{n-}\cdots SH_2 \overset{h\nu}{\rightleftharpoons} [P^{n-}\cdots SH_2]^* \quad \text{(photoexitation)} \quad (2)$$

$$[P^{n-}\cdots SH_2]^* \overset{k_{ET}}{\rightleftharpoons} P^{(n+1)-} + SH^\bullet + H^+ \quad \text{(electron transfer)} \quad (3)$$

$$P^{(n+1)-} + SH^\bullet \rightarrow P^{(n+2)-} + S + H^+ \quad \text{(radical reaction)} \quad (4)$$

$$2P^{(n+2)-} + O_2 + 4H^+ \rightarrow 2P^{n-} + 2H_2O \quad \text{(oxidation)} \quad (5)$$

$$P^{(n+2)-} + 2H^+ \rightarrow P^{n-} + H_2 \quad \text{(oxidation)} \quad (6)$$

Equation 1 represents formation of the electron-donor−acceptor complex with rate constant k_{EDA}. Light is represented by $h\nu$, and k_{ET} is the electron-transfer rate constant. Regeneration by O_2 (eq 5) may generate a number of reduced oxygen species (H_2O, H_2O_2, HO_2).[8d] The emphasis in most of the studies described to date has been on the efficiency of the steps leading to substrate oxidation (eq 1−3) rather than on the nature and role of the reduced forms of the cluster anions (eqs 3, 5, and 6).

Electrochemical studies have established that many polyoxometalate anions can undergo a series of reversible redox cycles involving electron- and proton-transfer reactions.[1h,9] The present work has investigated systematically the nature and reactions of reduced forms of the anions $[S_2M_{18}O_{62}]^{4-}$ (M = W,[9a,10] Mo[9b,11]) and $[SMo_{12}O_{40}]^{2-}$[9c,12] using in situ voltammetric techniques. At the same time, the concept of electrolytic regeneration of the photocatalysts (eq 7) has been examined as an alternative to the O_2/H^+ regeneration pathways (eqs 5 and 6), which are often thermodynamically or kinetically unfavorable.

$$P^{(n+2)-} \rightarrow P^{n-} + 2e^- \quad (7)$$

The use of voltammetric techniques has allowed a detailed study of the nature and redox chemistry of the anions to be undertaken at low concentrations during the course of photochemical reactions with organic substrates, and consequently their potential as homogeneous oxidation catalysts has been evaluated for the first time.

Experimental Section

Reagents. Acetone (Aldrich, HPLC grade, 99.9+%), acetonitrile (Merck, HPLC grade, 99.9%), benzyl alcohol (BDH), benzaldehyde, ethanol (BDH, 95−96%), (−)-menthol (Aldrich), and ferrocene (BDH) were used as supplied by the manufacturers. The electrolytes, tetrahexylammonium hexafluorophosphate (Hex_4NPF_6) and tetrabutylammonium hexafluorophosphate (Bu_4NPF_6), were prepared as described in ref 13a. The polyoxometalates, $[Bu_4N]_4[S_2W_{18}O_{62}]$,[9a] $[Hex_4N]_4[S_2Mo_{18}O_{62}]$,[9b] $[Hex_4N]_2[SMo_{12}O_{40}]$,[12a] $[Hex_4N]_6[P_2W_{18}O_{62}]$,[8b] and $[Bu_4N]_3[PW_{12}O_{40}]$,[5e] were synthesized according to procedures reported in the literature.

Instrumentation and Procedures. Solution-phase voltammetric experiments using stationary macrodisk electrodes were carried out in a standard three-electrode arrangement with a glassy carbon (GC) disk

(4) (a) Neumann, R. In *Transition Metals for Organic Synthesis*; Beller, M., Bolm, C., Eds.; Wiley-VCH: Weinheim, 1998; Vol. 2, p 331. (b) Anderson, T. M.; Hardcastle, K. I.; Okun, N.; Hill, C. L. *Inorg. Chem.* **2001**, *40*, 6418. (c) Neumann, R.; Abu-Gnim, C. *J. Am. Chem. Soc.* **1990**, *112*, 6025. (d) Faraj, M.; Hill, C. L. *J. Chem. Soc., Chem. Commun.* **1987**, 1487. (e) Hill, C. L.; Brown, R. B. *J. Am. Chem. Soc.* **1986**, *108*, 536.

(5) (a) Hiskia, A.; Mylonas, A.; Papaconstantinou, E. *Chem. Soc. Rev.* **2001**, *30*, 62. (b) Hill, C. L.; Prosser-McCartha, C. M. In *Photosensitization and Photocatalysis Using Inorganic and Organometallic Complexes*; Kalyanasundaram, K., Gräzel, M., Eds.; Kluwer Academic Publishers: Dordrecht, The Netherlands, 1993; Chapter 13, p 307. (c) Renneke, R. F.; Pasquali, M.; Hill, C. L. *J. Am. Chem. Soc.* **1990**, *112*, 6585. (d) Sattari, D.; Hill, C. L. *J. Chem. Soc., Chem. Commun.* **1990**, 634. (e) Hill, C. L.; Buchard, D. A. *J. Am. Chem. Soc.* **1985**, *107*, 5148.

(6) (a) Duncan, D. C.; Chambers, R. C.; Hecht, E.; Hill, C. L. A. *J. Am. Chem. Soc.* **1995**, *117*, 681. (b) Ballistreri, F. P.; Tomaselli, G. A.; Toscano, R. M.; Conte, V.; Di Furia, F. *J. Mol. Catal.* **1994**, *89*, 295. (c) Salles, L.; Aubry, C.; Thouvenot, R.; Robert, F.; Dorémieux-Morin, C.; Chottard, G.; Ledon, H.; Jeanin, Y.; Brégeault, J.-M. *Inorg. Chem.* **1994**, *33*, 871. (d) Salles, L.; Aubry, C.; Robert, F.; Chottard, G.; Thouvenot, R.; Ledon, H.; Brégeault, J.-M. *New J. Chem.* **1993**, *17*, 367. (e) Aubry, C.; Chottard, G.; Platzer, N.; Brégeault, J.-M.; Thouvenot, R.; Chauveau, F.; Huet, C.; Ledon, H. *Inorg. Chem.* **1991**, *30*, 4409. (f) Dengel, A. C.; Griffith, W. P.; Parkin, B. C. *J. Chem. Soc., Dalton Trans.* **1993**, 2683.

(7) (a) Khenkin, A. M.; Hill, C. L. *Mendeleev Commun.* **1993**, 140. (b) Neumann, R.; Gara, M. *J. Am. Chem. Soc.* **1995**, *117*, 5066. (c) Neumann, R.; Khenkin, A. M.; Juwiler, D.; Miller, H.; Gara, M. *J. Mol. Catal.* **1997**, *117*, 169. (d) Mizuno, N.; Nozaki, C.; Kiyoto, I.; Misono, M. *J. Am. Chem. Soc.* **1998**, *120*, 9267. (e) Zhang, Z.; Chen, Q.; Duncan, D. C.; Lachicotte, R. J.; Hill, C. L. *Inorg. Chem.* **1997**, *36*, 4381. (f) Zhang, X.; Chen, Q.; Duncan, D. C.; Campana, C. F.; Hill, C. L. *Inorg. Chem.* **1997**, *36*, 4208. (g) Ben-Daniel, R.; Khenkin, A. M.; Neumann, R. *Chem. Eur. J.* **2000**, *6*, 3722.

(8) (a) Harrup, M. K.; Hill, C. L. *Inorg. Chem.* **1994**, *33*, 5448. (b) Hiskia, A.; Papaconstantinou, E. *Inorg. Chem.* **1992**, *31*, 163. (c) Neumann, R.; Levin, M. *J. Am. Chem. Soc.* **1992**, *114*, 7278. (d) Duncan, D. C.; Hill, C. L. *J. Am. Chem. Soc.* **1997**, *119*, 243. (e) Khenkin, A.; Neumann, R. *Angew. Chem, Int. Ed.* **2000**, *39*, 4088. (f) Khenkin, A.; Weiner, L.; Wang, Y.; Neumann, R. *J. Am. Chem. Soc.* **2001**, *123*, 8531.

(9) (a) Richardt, P. J. S.; Gable, R. W.; Bond, A. M.; Wedd, A. G. *Inorg. Chem.* **2001**, *40*, 703. (b) Way, D. M.; Bond, A. M.; Wedd, A. G. *Inorg. Chem.* **1997**, *36*, 2826. (c) Maeda, K.; Himeno, S.; Osakai, T.; Saito, A.; Hori, T. *J. Electroanal. Chem.* **1994**, *364*, 149 and references cited therein. (d) Himeno, S.; Maeda, K.; Osakai, T.; Saito, A.; Hori, T. *Bull. Chem. Soc. Jpn.* **1993**, *66*, 109 and references cited therein. (e) Casan-Pastor, N.; Baker, L. C. W. *J. Am. Chem. Soc.* **1992**, *114*, 10384. (f) Piepgrass, K.; Barrows, J. M.; Pope, M. T. *J. Chem. Soc., Chem. Commun.* **1989**, 10. (g) Harmalker, S. P.; Leparulo, M. A.; Pope, M. T. *J. Am. Chem. Soc.* **1983**, *105*, 4286. (h) Kozik, M.; Hammer, C. F.; Baker, L. C. W. *J. Am. Chem. Soc.* **1986**, *108*, 7627 and references cited therein.

(10) Himeno, S.; Tatewaki, H.; Hashimoto, M. *Bull. Chem. Soc. Jpn.* **2001**, *74*, 1623.

(11) (a) Hori, T.; Himeno, S. *Chem. Lett.* **1987**, 53. (b) Himeno, S.; Saito, A.; Hori, T. *Bull. Chem. Soc. Jpn.* **1989**, *62*, 2184. (c) Hori, T.; Tamada, O.; Himeno, S. *J. Chem. Soc., Dalton Trans.* **1989**, 1491.

(12) (a) Vu, T.; Bond, A. M.; Hockless, D. C. R.; Moubaraki, B.; Murray, K. S.; Lazarev, G.; Wedd, A. G. *Inorg. Chem.* **2001**, *40*, 65. (b) Hori, T.; Himeno, S.; Tamada, O. *J. Chem. Soc., Dalton Trans.* **1996**, 2083. (c) Himeno, S.; Miyashita, K.; Saito, A.; Hori, T. *Chem. Lett.* **1990**, 799.

(13) (a) Fry, A. J. In *Laboratory Techniques in Electroanalytical Chemistry*, 2nd ed.; Kissinger P. T., Heineman, W. R., Eds.; Marcel Dekker: New York, 1996; p 481. (b) Hussey, C. L. In *Laboratory Techniques in Electroanalytical Chemistry*, 2nd ed.; Kissinger P. T., Heineman, W. R., Eds.; Marcel Dekker: New York, 1996; p 529.

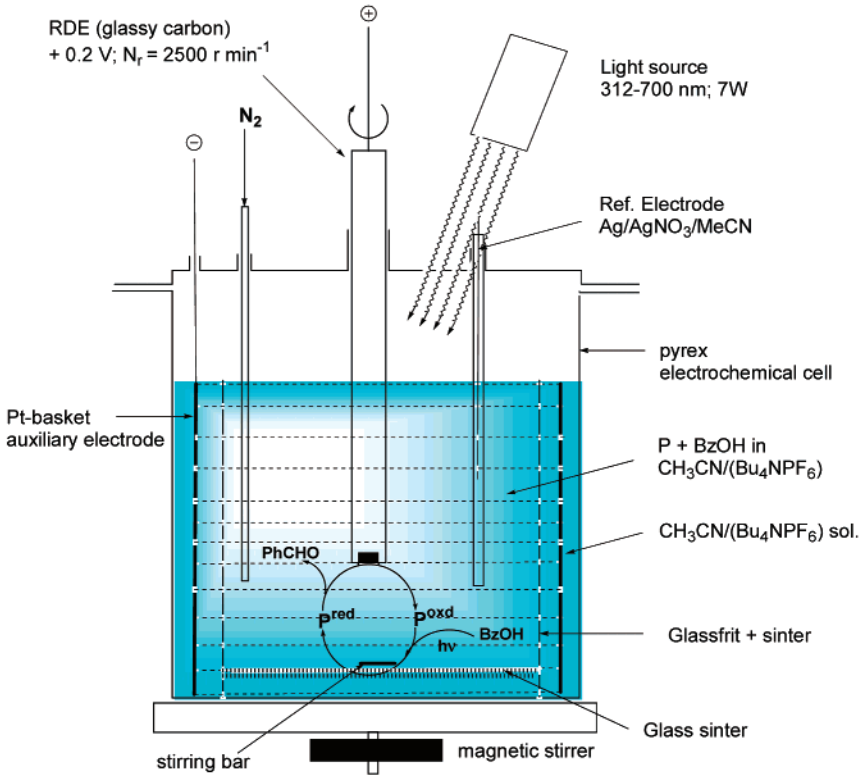

Figure 1. Apparatus used in photooxidation reaction experiments when a GC rotating disk working electrode is used for catalyst regeneration.

working electrode, a platinum wire as the counter electrode, and an Ag/Ag^+ (MeCN, 10 mM $AgNO_3$) double-junction reference electrode. Unless otherwise stated, experiments were conducted at ambient temperature (20 ± 3 °C) under nitrogen. The glassy carbon electrode area of 0.071 cm^2 was determined by measurement of the peak current value obtained for reversible one-electron oxidation of a 1 mM solution of ferrocene by cyclic voltammetry and the Randles−Sevcik equation,[13b]

$$I_p = 0.4463(n^{3/2}F^{3/2}/R^{1/2}T^{1/2})AD^{1/2}C\nu^{1/2} \quad (8)$$

where I_p is the peak current (A), n is the number of electrons, A is the electrode area (cm^2), D is the diffusion coefficient (taken to be 2.3×10^{-5} cm^2 s^{-1}), C is the concentration (mol cm^{-3}), ν is the scan rate (V s^{-1}), and the other symbols have their usual meaning. Electrode potentials are quoted relative to the Ag/Ag^+ or the ferrocenium/ferrocene redox couple (Fc^+/Fc; $E_{(Fc/Fc^+)} = E_{(Ag/Ag^+)} - 0.1$ V). Rotating disk electrode (RDE) experiments used the same electrode configuration as for stationary solution ones, except that the glassy carbon disk working electrode was rotated by a variable-speed rotator (Metrohm 628-10).

In one configuration, polyoxometalate catalyst regeneration experiments using in situ electrolytic oxidation at a constant direct current (dc) potential were carried out in Pyrex cells using a cylindrical platinum gauze basket counter electrode which was separated from the test solution by a porous glass sinter, a GC rotating disk working electrode, and the same reference electrode as employed in the voltammetric experiments (Figure 1). Alternatively, electrochemical regeneration of the catalyst was achieved by a large surface area Pt gauze basket placed in the working electrode compartment of the cell shown in Figure 1. In either configuration, voltammetric monitoring of the course of these bulk electrolysis regeneration experiments was undertaken using the rotating disk electrode, and light was introduced from the top of the cell.

Detection of photocurrents associated with oxidation of photoreduced cluster anions was undertaken using the "thin-layer" solution cell design shown in Figure 2. In this case, light was introduced from the bottom

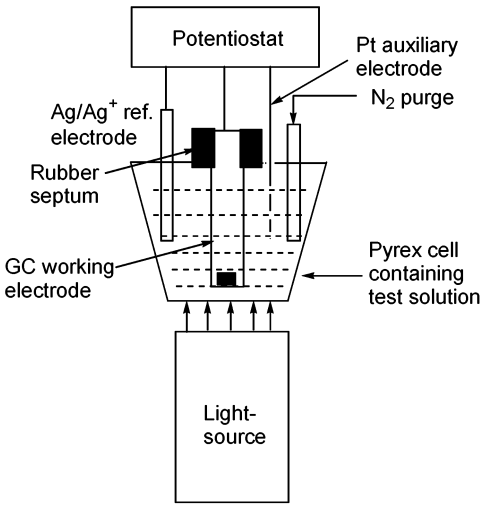

Figure 2. Schematic diagram of the experimental arrangement used in the thin-layer photoelectrochemical experiments.

of the electrochemical cell, and the solution layer thickness was used at a constant value. The same cell was used in each experiment. The photochemical currents were detected voltammetrically in a 2-mm layer of solution with a stationary GC electrode held at a constant dc potential.

Irradiation of samples with light at 312−700 nm or at specific wavelengths was achieved using a Polilight PL6 (Rofin) light source fitted with filters and a flexible liquid light guide. The total power output of the lamp at the end of the liquid light guide was, according to the manufacturer's specification, 7 (at 312−700 nm), 0.37 (340 nm), 0.48 (425 nm), 0.82 (450 nm), 0.58 (505 nm), and 0.54 W (530 nm). Use of light in the visible range of 312−700 nm allows the photochemically induced reactions of $[Hex_4N]_2[SMo_{12}O_{40}]$, $[Bu_4N]_4[S_2W_{18}O_{62}]$, and $[Hex_4N]_4[S_2Mo_{18}O_{62}]$ to be conveniently undertaken in cells constructed from Pyrex glassware. A few experiments were undertaken with a

Table 1. Reversible Half-Wave Potentials ($E_{1/2}$, mV vs Fc^+/Fc^0)[a] Determined by Voltammetric Techniques for the First Four Reduction Processes (1 mM MeCN Solutions) of $[SMo_{12}O_{40}]^{2-}$ (0.1 M Hex_4NClO_4), $[S_2Mo_{18}O_{62}]^{4-}$ (0.1 M Bu_4NPF_6), and $[S_2W_{18}O_{62}]^{4-}$ (0.1 M Bu_4NClO_4)[b]

	process 1	$E_{1/2}$ (mV)	process 2	$E_{1/2}$ (mV)	process 3	$E_{1/2}$ (mV)	process 4	$E_{1/2}$ (mV)
1a	$[S_2W_{18}O_{62}]^{4/5-}$	−235	$[S_2W_{18}O_{62}]^{5/6-}$	−615	$[S_2W_{18}O_{62}]^{6/7-}$	−1180	$[S_2W_{18}O_{62}]^{7/8-}$	−1570
1b	$[S_2Mo_{18}O_{62}]^{4/5-}$	+100	$[S_2Mo_{18}O_{62}]^{5/6-}$	−135	$[S_2Mo_{18}O_{62}]^{6/7-}$	−795	$[S_2Mo_{18}O_{62}]^{7/8-}$	−1070
2	$[SMo_{12}O_{40}]^{2/3-}$	+230	$[SMo_{12}O_{40}]^{3/4-}$	−190	$[SMo_{12}O_{40}]^{4/5-}$	−790	$[SMo_{12}O_{40}]^{5/6-}$	−1370

[a] See refs 9a (**1a**), 9b (**1b**), and 12a (**2**) for details. [b] GC electrode (3 mm); $\nu = 100$ mV s^{-1}.

conventional high-power (1000 W) light source in a Rayonet reactor (Southern New England Ultraviolet Corp.) in order to increase the rate of photolysis.

The products of photooxidation were identified by gas chromatography (Varian 3700; fused silica capillary column 30 QC 5/BP x 5 and packed-column Carbowax 20% SE 30) using anisole as an internal standard and GC/MS (Agilent 6890 series (GC), Agilent 5973 Network mass-selective detector (MS); HP 5 MS cross-linked 5% PH ME siloxane column, 30 m × 0.25 mm × 0.25 μm).

Photoelectrochemical voltammetry experiments were carried out using a Voltalab PGZ 301 (Radiometer) electrochemical system. A BAS100B (Bioanalytical Systems) electrochemical workstation or a Cypress Systems (model CYSY-1R) computer-controlled electroanalysis system was used in other voltammetric experiments.

Results and Discussion

Redox Processes. Recent voltammetric studies have shown that $[R_4N]_4[S_2M_{18}O_{62}]$ {M = W, R = Bu (**1a**);[9a] M = Mo, R = Hex (**1b**)[9b,d,11b,14]} and $[Hex_4N]_2[SMo_{12}O_{40}]$ (**2**)[9c,12a] undergo a series of highly reversible (pH-dependent) reduction processes (eq 9a,b) and that salts of intensely colored $1e^-$ (green or blue)- and $2e^-$ (blue)-reduced products can be isolated in substance by bulk electrolysis.[12a,14a,15]

$$\underset{\text{yellow}}{[SMo_{12}O_{40}]^{2-}} \overset{+e^-}{\underset{-e^-}{\rightleftharpoons}} \underset{\text{green}}{[SMo_{12}O_{40}]^{3-}} \overset{+e^-}{\underset{-e^-}{\rightleftharpoons}} \underset{\text{blue}}{[SMo_{12}O_{40}]^{4-}} \overset{+e^-}{\underset{-e^-}{\rightleftharpoons}} [SMo_{12}O_{40}]^{5-} \overset{+e^-}{\underset{-e^-}{\rightleftharpoons}} [SMo_{12}O_{40}]^{6-} \quad (9a)$$

$$\underset{\text{orange}}{[S_2M_{18}O_{62}]^{4-}} \overset{+e^-}{\underset{-e^-}{\rightleftharpoons}} \underset{\substack{\text{green (M = Mo)}\\ \text{blue (M = W)}}}{[S_2M_{18}O_{62}]^{5-}} \overset{+e^-}{\underset{-e^-}{\rightleftharpoons}} \underset{\text{blue}}{[S_2M_{18}O_{62}]^{6-}} \overset{+e^-}{\underset{-e^-}{\rightleftharpoons}} [S_2M_{18}O_{62}]^{7-} \overset{+e^-}{\underset{-e^-}{\rightleftharpoons}} [S_2M_{18}O_{62}]^{8-} \quad (9b)$$

where M = Mo, W

Table 1 summarizes the reversible potentials versus Fc^+/Fc^0 for the first four one-electron processes observed in MeCN for **1** and **2**. The Dawson anion **1a** is much harder to reduce than its Mo analogue **1b** or the Keggin anion **2**. However, this also implies that the reduced forms of **1a** will be easier to oxidize to the starting ion, which is favorable for a catalytic cycle. Upon irradiation with light, the photoexcited-state redox potentials of **1a** and other polyoxometalates have been shown to become considerably more positive compared to the dark ground state.[1i,5a,16] As will be shown in this study, **1b** and **2** also exhibit this property, rendering each anion a suitable agent for the photooxidation of organic substrates, for which rates of oxidation are limited in the absence of light.

Table 2. Oxidative Photocurrents,[a] *I*, for **1**, $[P_2W_{18}O_{62}]^{6-}$, $[PW_{12}O_{40}]^{3-}$, and **2** and Substrates (0.1 M) upon Irradiation with 7-W Light of Wavelength 312−700 nm

	I (μA)		
anion	BzOH	EtOH	MentOH
1a[b]	0.79	0.12	0.27
1b[b]	0.45	0.20	0.38
2[c]	4.0	0.29	0.31
$[P_2W_{18}O_{62}]^{6-}$ [b]	0.08	*d*	*d*
$[PW_{12}O_{40}]^{3-}$ [b]	0.14	*d*	*d*

[a] Data obtained in the thin-layer electrochemical cell configuration shown in Figure 2. [b] 0.5 mM polyoxometalate anion in MeCN (0.1 M Bu_4NPF_6). [c] 0.5 mM polyoxometalate anion in acetone (0.1 M Hex_4NPF_6). [d] Not determined.

Numerous reports describe the catalytic application of polyoxometalates (mainly phospho-Keggin anions $[PM_{12}O_{40}]^{q-}$).[1d,e,g,2,5c−e] The photoexited states of **1** and **2** are promising candidates for photochemical oxidations, and preliminary studies are available.[17] In the present work, **1** and **2** were examined as catalysts for the photooxidation of benzyl alcohol (BzOH) ($E_p^{ox} = 2.12$ V), ethanol (EtOH) ($E_p^{ox} = 3.0$ V, shoulder), and (−)-menthol (MentOH) ($E_p^{ox} = 2.4$ V).[18] The irreversible peak potential for the oxidation E_p^{ox} values quoted above are considerably more positive than the ground-state reversible potentials of the anions (Table 1).

Initial Experiments. MeCN or acetone solutions (0.1 M Bu_4NPF_6) of the anions (0.5 mM) and the organic substrates (100 mM) were exposed to light in the electrochemical cell thin-layer solution configuration shown in Figure 2. To measure the photocurrent, the potential of the GC working electrode was set more positive than the reversible values of the anions (Table 1) but less positive than the electrochemical oxidation potentials of the substrates discussed above. In each experiment, dark and illuminated periods were of 2−2.5 min duration. The currents listed in Tables 2 and 3 are estimated from the intersection of straight-line plots obtained from the initial steep rise in photocurrent (20−60 s) and the slowly rising section of the current−time plot obtained after the initial steeply rising period until the light was switched off. As expected, at this potential no current was detected in the absence of light, but the current flow detected when the light was switched on (Figure 3a) indicated that photooxidation of the substrate occurred with concomitant reduction of the anion. For comparative purposes,

(14) (a) Way, D. M.; Cooper, J. B.; Sadek, M.; Vu, T.; Mahon, P. J.; Bond, A. M.; Brownlee, R. T. C.; Wedd, A. G. *Inorg. Chem.* **1997**, *36*, 4227. (b) Cooper, J. B.; Bond, A. M.; Oldham, K. B. *J. Electroanal. Chem.* **1992**, *331*, 877. (c) Himeno, S.; Osakai, T.; Saito, A.; Maeda, K.; Hori, T. *J. Electroanal. Chem. Interfacial Electrochem.* **1992**, *337*, 371.
(15) (a) Richardt, P. J. S.; White, J. M.; Tregloan, P. A.; Bond, A. M.; Wedd, A. *Can. J. Chem.* **2001**, *79*, 613. (b) Cooper, J. B.; Way, D. M.; Bond, A. M.; Wedd, A. G. *Inorg. Chem.* **1993**, *32*, 2416.
(16) Balzani, V.; Bolletta, F.; Gandolfi, M. T.; Maestri, M. *Top. Curr. Chem.* **1978**, *75*, 1.
(17) (a) Eklund, J. C.; Bond, A. M.; Humphrey, D. G.; Lazarev, G.; Vu, T.; Wedd, A. G.; Wolfbauer, G. *J. Chem. Soc., Dalton Trans.* **1999**, 4373. (b) Bond, A. M.; Eklund, J. C.; Tedesco, V.; Vu, T.; Wedd, A. G. *Inorg. Chem.* **1998**, *37*, 2366. (c) Bond, A. M.; Way, D. M.; Wedd, A. G.; Compton, R. G.; Booth, J.; Eklund, J. C. *Inorg. Chem.* **1995**, *34*, 3378.
(18) Peak potential data vs Fc^+/Fc by voltammetry at a GC electrode in MeCN (0.1 M Bu_4NPF_6) using a scan rate of 100 mV s^{-1}.

Table 3. Wavelength-Dependent Photocurrents,[a] I_{nm}, for **1**, $[P_2W_{18}O_{62}]^{6-}$, $[PW_{12}O_{40}]^{3-}$,[b] and **2**[c] and Organic Substrates (0.1 M)

anion/substrate	I_{340}/nA W^{-1}	I_{425}/nA W^{-1}	I_{450}/nA W^{-1}	I_{505}/nA W^{-1}	I_{530}/nA W^{-1}	λ_{max}[e]/nm
1a/BzOH	592	[d]	315	440	433	252, 300 (sh)
1b/BzOH	243	79	193	243	191	217, 310 (sh)
2/BzOH	1935	823	1098	1414	1281	315
$[P_2W_{18}O_{62}]^{6-}$/BzOH	24	*d*	ca. 9	ca. 9	<9	255, 294 (sh)
$[PW_{12}O_{40}]^{3-}$/BzOH	59	*d*	ca. 12	ca. 12	<9	265
1a/EtOH	54	<10	70	90	74	
1b/EtOH	87	42	77	116	122	
2/EtOH	211	*d*	106	124	102	
1a/MentOH	130	ca. 10	55	79	76	
1b/MentOH	192	*d*	63	52	39	
2/MentOH	181	ca. 19	146	176	137	

[a] Obtained in the cell shown in Figure 2. [b] 0.5 mM in MeCN, Bu_4NPF_6 (0.1 M). [c] 0.5 mM in acetone, Hex_4NPF_6 (0.1 M). [d] Below detection limit. [e] Literature values of O−M charge-transfer bands in the absence of substrate: **1a**, ref 20; **1b**, refs 11a, 14a; **2**, ref 12c; $[P_2W_{18}O_{62}]^{6-}$ and $[PW_{12}O_{40}]^{3-}$, ref 1i.

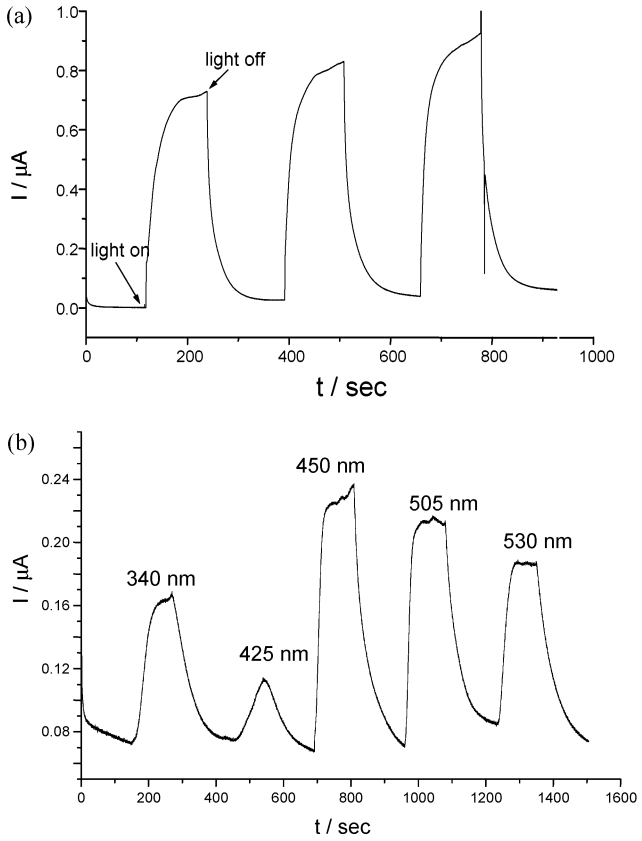

Figure 3. Oxidative photocurrents obtained in the thin-layer electrochemical cell configuration depicted in Figure 2, with a 3-mm GC electrode held at a potential of 0.2 (**1a**) and 0.4 V (**1b**) (vs Ag/Ag$^+$), respectively. (a) For **1a**, $\lambda = 312-700$ nm at 7 W. (b) For **1b** at specific wavelengths and light intensities (see Experimental Section). Anion and benzyl alcohol concentrations in MeCN (0.1 M Bu_4NPF_6) were 0.5 and 100 mM, respectively.

photocurrents in the presence of the well-known anions $[P_2W_{18}O_{62}]^{6-}$ and $[PW_{12}O_{40}]^{3-}$ also were measured under the same conditions.

The magnitude of oxidative photocurrents (I_{ox}) detected in the thin-layer configuration represents a large fraction of the reduction currents (I_{red}), detected when a constant dc potential was applied at a value corresponding to the limiting current region of the reduction process in the dark ($I_{ox}/I_{red} = 0.65$ (**1a**), 0.59 (**1b**), 0.5 (**2**)). This implies that extensive photoconversion to the one-electron or more highly reduced form of the anions occurred under these thin-layer conditions.

Significantly larger photocurrents were always observed (Table 2) for BzOH relative to primary and secondary aliphatic alcohols, consistent with the relative ease of oxidation of BzOH.[19] Data for photocurrent magnitudes obtained at different wavelengths (for the same solutions) are summarized in Table 3, with a representative data set for BzOH/**1b** displayed in Figure 3b. Examination of the data reveals that all of the sulfo anions exhibit significant photocurrents in all of the visible region ($\lambda = 340-530$ nm), which implies that light absorbance by highly colored reduced forms also contributes to the photocurrent. The sulfo anions also show considerably greater photocurrents than the phospho anions in the visible region ($\lambda = 450-530$ nm), which explains why much smaller photocurrents are obtained relative to the case when the sulfo anions are irradiated with light encompassing the wavelengths of most of the visible region (312−700 nm, Table 2).

Voltammetric Monitoring of the Photooxidation of Benzyl Alcohol with 1a under Anaerobic Conditions. Equation 10 formally describes the two-electron oxidation of BzOH to benzaldehyde, assuming that **1a** acts as a 2e$^-$ acceptor and that the reduced anion binds the liberated protons (eqs 3 and 4). For catalysis to proceed (eq 11) under these conditions, **1a** must be regenerated via eq 12.

$$C_6H_5CH_2OH + [S_2W_{18}O_{62}]^{4-} \xrightarrow{h\nu} C_6H_5CHO + [S_2W_{18}O_{60}(OH)_2]^{4-} \quad (10)$$

$$C_6H_5CH_2OH \xrightarrow{h\nu} C_6H_5CHO + H_2 \quad (11)$$

$$[S_2W_{18}O_{60}(OH)_2]^{4-} \rightarrow [S_2W_{18}O_{62}]^{4-} + H_2 \quad (12)$$

Conversion of substrate to benzaldehyde was followed by gas chromatography, while the fates of **1a** and H^+ were monitored by rotating disk electrode voltammetry (RDEV) and cyclic voltammetry (CV) over the potential ranges from +0.15 to −1.0 V and from 1.2 to −2.2 V vs Ag/Ag$^+$, respectively. Changes in the polyoxometalate redox state were reflected in RDEV experiments by noting the position of the limiting current plateaux relative to zero current, I_o (Figure 4), while the magnitude of the limiting current determined the concentration. Information on the net concentration of the hydrogen ions generated in eq 10 and consumed in eq 12 can be obtained from

(19) Appropriate blank experiments confirmed that (i) the solvents are not photooxidized, (ii) redox reactions do not occur in the dark, and (iii) anodic photocurrents are not detected in the absence of substrates.

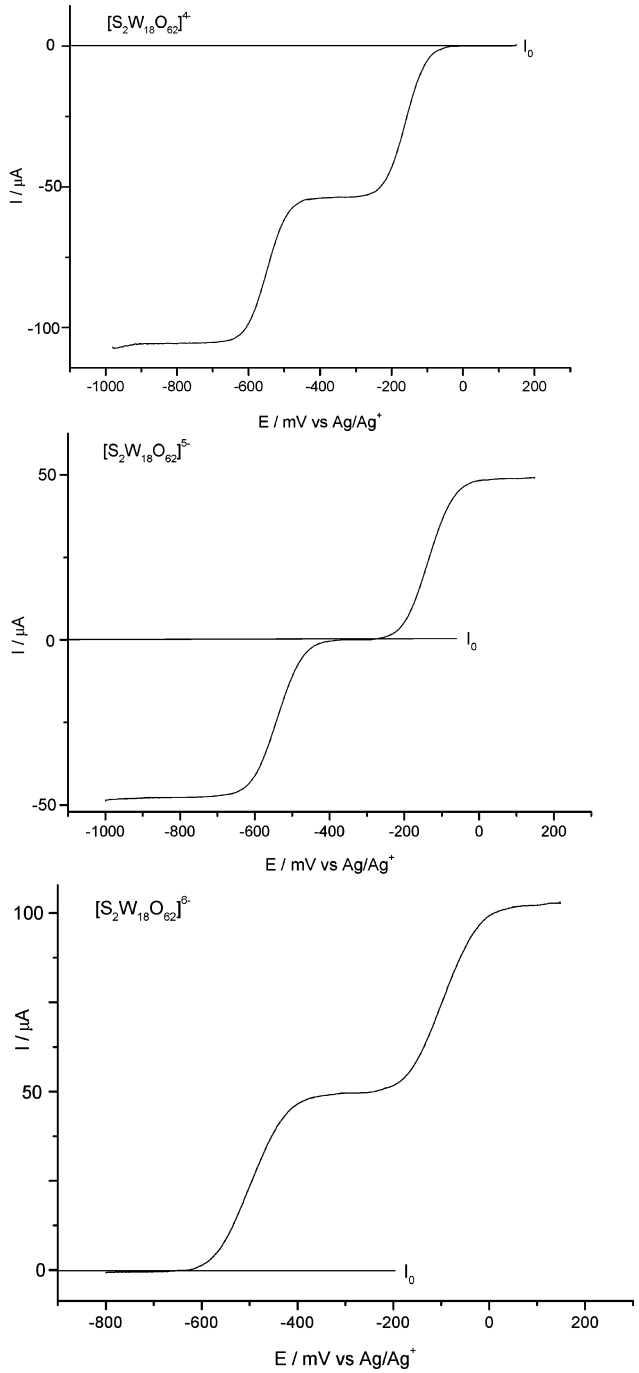

Figure 4. Position of zero current, I_0, in RDE voltammograms obtained at a GC electrode from MeCN (0.1 M Bu_4NPF_6) solutions containing 1.6 mM $[S_2W_{18}O_{62}]^{n-}$. $\nu = 10$ mV s^{-1}, $N_r = 1000$ rpm.

the potential at which various polyoxometalate processes are detected and from the shapes of voltammetric waves when protons are present.

The influence of hydrogen ion concentration on the voltammetry of the anions in MeCN/water (95:5) has been reported previously.[9a−e,14] Addition of acid causes the first four reversible 1e$^-$ processes observed for **1b**[9b] to coalesce into two reversible, overall 2e$^-$ processes at more positive potentials. Similar behavior occurs for the third and fourth 1e$^-$ processes of **1a**.[9a] As a consequence of the hydrogen ion concentration dependence and the different basicisity of **1a**,**b**, complex redox/protonation equilibria exist for each system.[9a,14a] To obtain reference data

Scheme 1

$$[S_2W_{18}O_{62}]^{4-} + e^- \rightleftharpoons [S_2W_{18}O_{62}]^{5-} + e^- \rightleftharpoons [S_2W_{18}O_{62}]^{6-}$$

$$H^+ \downarrow\uparrow \qquad\qquad H^+ \downarrow\uparrow$$

$$[S_2W_{18}O_{61}(OH)]^{4-} + e^- \rightleftharpoons [S_2W_{18}O_{61}(OH)]^{5-}$$

$$H^+ \downarrow\uparrow$$

$$[S_2W_{18}O_{60}(OH)_2]^{4-}$$

in neat MeCN (0.08 mM Bu_4NPF_6), voltammetric studies of **1a** (0.9 mM) as a function of CF_3SO_3H concentrations (0.18−3.6 mM) were conducted (see Figures 5 and S1).[21] After the addition of approximately 0.68 mM of CF_3SO_3H, the first two 1e$^-$ reductions converted into a reversible 2e$^-$ process at a more positive potential. In the presence of 1 mol equiv of acid, the RDEV exhibits two fully developed 2e$^-$ reduction processes followed by a third less developed process, which also becomes a 2e$^-$ process upon further addition of acid. A cyclic voltammogram scanned over the potential range from +1.5 to −1.5 V ($\nu = 500$ mV s^{-1}) in the presence of ≥1.8 mM of acid exhibits three chemically reversible redox processes at significantly more positive potentials (40−247 mV) than in the absence of acid (Figure S1). Reduction waves at more negative potentials also coalesce into multielectron processes.

The proton concentration dependence in neat MeCN differs from that reported in MeCN/water (95:5), where the first two redox couples remain as 1e$^-$ processes in the presence of 4 mol equiv of acid (**1a**: 1 mM; $HClO_4$: 4 mM).[9a] This difference implies that, in neat MeCN, the one- and two-electron-reduced anions $[S_2W_{18}O_{62}]^{5-}$ and $[S_2W_{18}O_{62}]^{6-}$ are relatively more basic and hence more readily protonated. Reaction Scheme 1, extended from earlier studies,[9a] can therefore be employed as a simple model to describe the acid-dependent behavior in neat MeCN.

The photooxidation of BzOH by **1a** was studied at a substrate-to-polyoxometalate concentration-ratio of BzOH:**1a** = 3:1 in deoxygenated MeCN solution (0.05 M Bu_4NPF_6) using the 312−700 nm visible light source. A low-intensity light source (7 W) was used to slow the rate of product formation so that catalyst regeneration pathways could be detected conveniently by voltammetric methods. Reference data (e.g., Figure 5) enabled the magnitude of currents and voltammetric wave shapes obtained during the course of the photochemical reaction to be interpreted in terms of redox level and concentration of the polyoxometalate as well as acid concentration.

The observed variation of oxidation currents as a function of time is shown in Figures 6 and 7. The shape, but not the position of zero current in the RDE voltammogram obtained after 26.5 h of irradiation (curve e in Figure 6A) is similar to that seen for **1a** (0.9 mM) alone after addition of 0.45 mM of acid (Figure 5). Due to partial reduction of **1a**, however, the maximum limiting current is detected at 188 μA in the range of 0−0.2 V vs Ag/Ag^+. These observations are consistent with initial reduction of **1a** and concomitant generation of H^+, as predicted by eq 10. Remarkably, during the course of the next 25 h of exposure to light, there was a decrease in oxidation

(20) Richardt, P. J. S. Ph.D. Thesis, University of Melbourne, Melbourne, Victoria, Australia, 2000.
(21) CF_3SO_3H behaves as a strong acid in MeCN: Fujinaga, T.; Sakamoto, I. *J. Electroanal. Chem.* **1977**, *85*, 185.

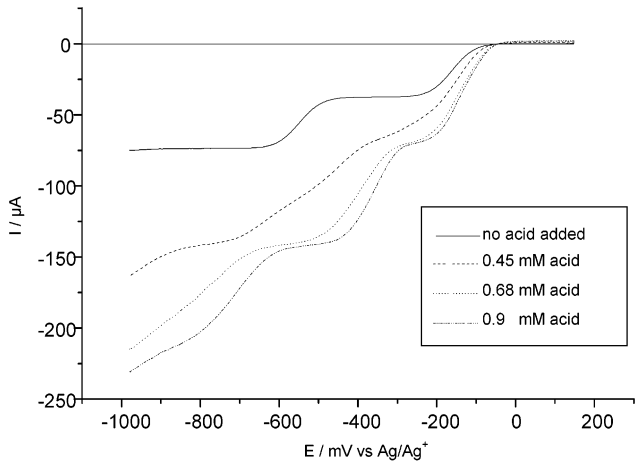

Figure 5. RDE voltammograms at a GC electrode after addition of CF_3SO_3H to $[S_2W_{18}O_{62}]^{4-}$ (0.9 mM) in MeCN (0.08 M Bu_4NPF_6). $\nu = 10$ mV s^{-1}, $N_r = 1000$ rpm.

current back toward zero (Figure 6B), consistent with reduced forms of **1a** being oxidized back to starting material. Furthermore, the wave shapes and the total magnitude of the (predominantly reduction) current ($I_T = -248$ μA, Figure 6B, $t =$ 46 h) were now similar to those observed for the purely reductive $1e^-$ processes at $t = 0$ ($I_T = -228$ μA, Figure 6A), consistent with the H^+ concentration being decreased. The voltammetric data indicate that, as the concentrations of H^+ and of reduced **1a** increase, the rates of eqs 13 and 14 increase (note their relationship to general eq 12 and to Scheme 1).

$$[S_2W_{18}O_{60}(OH)_2]^{4-} \rightarrow [S_2W_{18}O_{62}]^{4-} + H_2 \qquad (13)$$

$$[S_2W_{18}O_{61}(OH)]^{4-} \rightarrow [S_2W_{18}O_{62}]^{4-} + {}^1/_2H_2 \qquad (14)$$

Ultimately, it appears that protons generated from the oxidation of BzOH are consumed at a faster rate than they are generated via the photochemical pathway. The oxidation of reduced forms of **1a** via the related reduction with water have been suggested previously to explain the instability of the $2e^-$-reduced form $[S_2W_{18}O_{62}]^{6-}$ in MeCN solution.[9a]

Evidence for the existence of an oscillating sequence caused by the disparity in the relative rates of generation and loss of H^+ is provided by the color changes (eq 9b), by monitoring of I_{lim}^{ox} values as a function of time (Figure 7), and by wave shape analysis (Figure 6). However, while the concentrations of H^+ and both oxidized and reduced forms of **1a** oscillated, a steady conversion of BzOH into benzaldehyde occurred (Figure 7). The oscillating process continued until, after 200 h, the solution consisted of 53% benzaldehyde, 4% benzoic acid, and 43% unreacted BzOH.[22]

In summary, voltammetric data imply that, upon generation of sufficiently high concentrations of H^+, the oxidation processes in eq 13 and 14 occur at a sufficiently fast rate to lower the $[H^+]$ and regenerate photoactive **1a**, which in turn increases the rate of the photochemical process. Thus, due to the regeneration of **1a**, the reaction can be classified as catalytic. Voltammograms recorded during the course of the reaction revealed that the total voltammetric current, I_T, remained constant, as expected for quantitative reduction and oxidation cycles.

The value of the voltammetric method of monitoring the course of the photochemical process, as introduced in this study, is that it directly addresses the issues of (i) time-dependent changes in polyoxometalate redox levels, (ii) detection of the oxidation of reduced anions, and (iii) the role of the protons released during the dehydrogenation of BzOH and regeneration of the photocatalyst. This approach complements previous studies by NMR, IR, UV−vis, and labeling techniques,[5e,8,23] which addressed the nature of the oxidizing species, i.e., whether the cluster anions themselves, or rather fragments or isomers in equilibrium with the intact anion, were the active components. The voltammetric methods provide evidence that support the concept that the anions considered in this study remain intact during the course of the photooxidation of organic substrates, and that the role of the anions in the catalytic cycle involves changes which are related solely to variation in redox and protonation levels (eq 9, Scheme 1).

Oxidation of Reduced Polyoxometalate Anions by O_2 and H^+. The above study was conducted under a nitrogen atmosphere in order to restrict the catalyst regeneration pathway to reaction with protons (H_2 evolution, eq 6) rather than with O_2 (eq 5). Oxidation of reduced polyoxometalates by reaction with protons or O_2 has been reported in other studies where catalysis is observed.[1i,5e,8,23a,24] The data available from electronic spectroscopy, laser flash photolysis, and gas chromatographic techniques indicate that the ease with which the reoxidation takes place depends significantly on the class of the polyoxometalate anion involved. Oxidation of reduced polyoxovanadates and -molybdates by both H^+ and O_2 was found to be both thermodynamically and kinetically unfavorable, whereas reduced polyoxotungstates underwent facile oxidation.[5e] It is also clear from these studies that the O_2 pathway is generally faster than the H^+ pathway.[1i,5e,8b]

RDE voltammetry was used to study the redox behavior of the two-electron-reduced forms of anions (prepared by bulk electrolysis in MeCN solutions[12a,14a,15a]) in the presence of acid. In these experiments, stirred solutions (1.5−2 mM) containing between 1.5 and 4 mM CF_3SO_3H or HBF_4 (54 wt % in Et_2O) were either exposed to air or maintained under nitrogen. RDEV behavior was monitored ($\nu = 10$ mV s^{-1}; $N_r = 1000$ rpm) as a function of time. For the solutions containing the reduced Dawson **1b**($2e^-$) or Keggin **2**($2e^-$) anions, no change in the RDE limiting current data or wave shapes was observed over 24 h, either in the presence or in the absence of air (oxygen). This indicated that, under the specified conditions, oxidation of these $2e^-$-reduced anions according to the general equations 5 and 6 is either kinetically very slow or not thermodynamically viable. This result is in agreement with other studies on heteropolymolybdates.[5e,8b,24c]

In contrast, the dependence of both I_{lim}^{ox} and the wave shape on time demonstrated that **1a**($2e^-$) is oxidized slowly in the presence of both O_2 and H^+ under aerobic conditions (Figure

(22) We have detected formation of benzaldehyde by an unknown mechanism in blank experiments where MeCN solutions of BzOH have been irradiated in the absence of **1a**. However, this pathway is suppressed when the anions are present in solution.

(23) (a) Yamase, T.; Takabayashi, N.; Kaji, M. *J. Chem. Soc., Dalton Trans.* **1984**, 793. (b) Papaconstantinou, E.; Dimotikali, D.; Politou, A. *Inorg. Chim. Acta* **1980**, *46*, 155.

(24) (a) Argitis, P.; Papaconstantinou, E. *J. Photochem.* **1985**, *30*, 445. (b) Ioannidis, A.; Papaconstantinou, E. *Inorg. Chem.* **1985**, *24*, 439. (c) Papaconstantinou, E. *J. Chem. Soc., Chem. Commun.* **1982**, 12. (d) Akid, R.; Darwent, J. R. *J. Chem. Soc., Dalton Trans.* **1985**, 395.

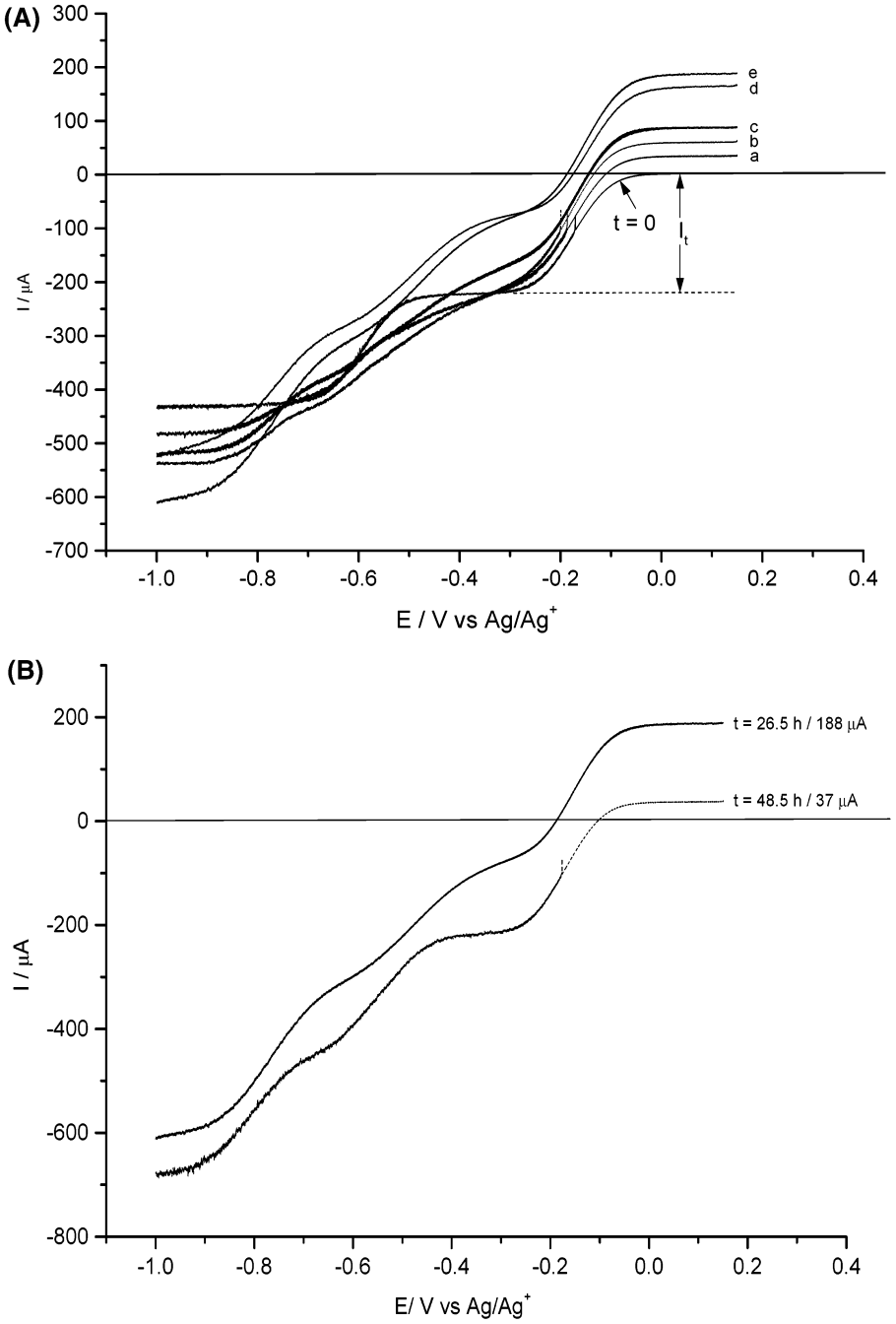

Figure 6. RDE voltammograms and limiting oxidative currents observed after BzOH (0.15 mmol) + $[S_2W_{18}O_{62}]^{4-}$ (0.05 mmol) in 10 mL of MeCN (0.05 M Bu_4NPF_6) was exposed to visible light ($\lambda = 312-700$ nm) for a designated period of time. $\nu = 10$ mV s^{-1}, $N_r = 1000$ rpm. (A) Voltammograms obtained during the period when **1a** was being reduced and $[H^+]$ was increasing. Reaction time and oxidative limiting current values were (a) 1 h/34 μA; (b) 2 h/60 μA; (c) 4 h/87 μA; (d) 21.5 h/165 μA; (e) 26.5 h/188 μA. (B) Voltammograms obtained during the period when **1a** was being recovered and $[H^+]$ was decreasing.

8A) and by H^+ only under anaerobic (Figure 8B) conditions. Analysis of RDE I_{lim}^{ox} vs time plots (Figure S2) indicates that the rate of aerobic oxidation is considerably faster than the rate of anaerobic oxidation, again consistent with observations on related systems.[1i,24d] The data obtained in the present study indicate clearly that the concentration of $[H^+]$ is important to both catalyst regeneration pathways.

Significantly, the rate of oxidation for **1a**($2e^-$) slows at the stage when the $1e^-$-reduced anion **1a**($1e^-$) is formed (Figure 8). Unlike **1a**($2e^-$), **1a**($1e^-$) appears to be stable under low-acidity conditions, in agreement with the stabilities of the isolated salts $[Bu_4N]_5[S_2W_{18}O_{62}]$ (stable) and $[Bu_4N]_6[S_2W_{18}O_{62}]$ (unstable).[15a]

Information relating to changes in $[H^+]$ again could be derived from analysis of the time dependence of the shapes of the RDE voltammetric curves. As oxidation of **1a**($2e^-$) proceeded, the initial wave shape found in the presence of acid, corresponding to an overall $2e^-$ process, slowly resolved into two well-separated $1e^-$ processes, similar to those observed under acid-free conditions (Figure 8), but with different positions of zero current. This clearly indicated that consumption of protons occurred consistent with eqs 5 and 6, respectively. The reaction

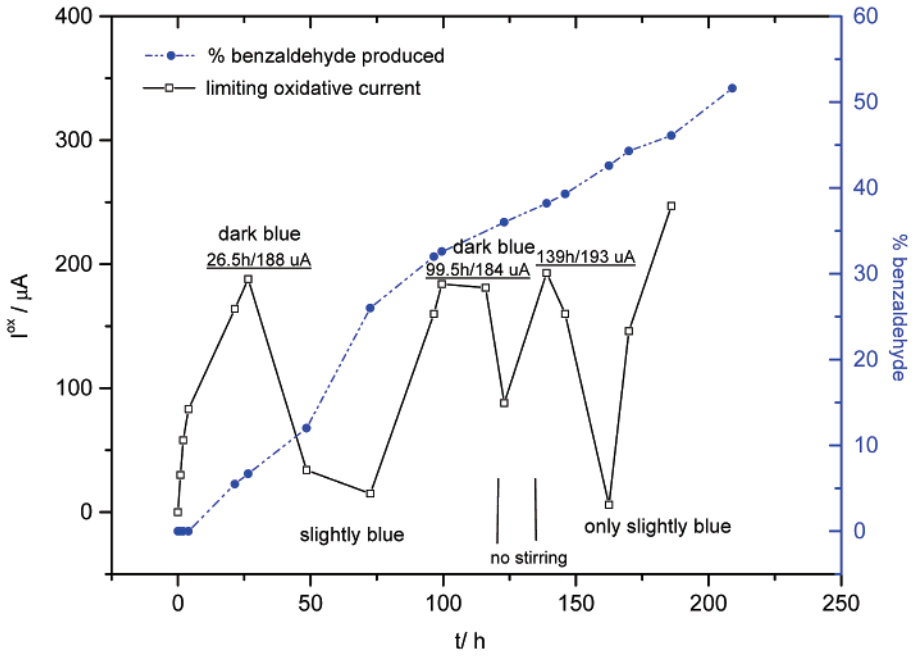

Figure 7. I_{ox} data at a GC electrode and % benzaldehyde formation as a function of time for the photooxidation of BzOH (0.15 mmol) in the presence of $[S_2W_{18}O_{62}]^{4-}$ (0.05 mmol) in 10 mL of MeCN (0.05 M Bu_4NPF_6) under N_2. $\lambda = 312-700$ nm, $\nu = 10$ mV s^{-1}, $N_r = 1000$ rpm.

pathway with HBF_4 (54 wt % in Et_2O) as a proton source under anaerobic conditions is shown in Figure S3 and even more clearly reveals transformation from a $2e^-$ process in the presence of acid to complete resolution into two well-separated $1e^-$ processes, as found for an acid-free medium. These experiments further support the view that an oxidation pathway for regeneration of catalyst involving consumption of protons and H_2 evolution (eq 12) is available.

Although the photochemical reaction between BzOH and **1a** presented in Figure 7 was conducted under a nitrogen atmosphere, oxidation of some reduced **1a** by trace amounts of air is possible. However, the low levels of benzoic acid detected by GC/MS indicate that this can be only a minor pathway.

Electrolytic Regeneration of the Catalyst. To establish an efficient catalytic cycle, rapid regeneration of the catalyst is crucial. In the case of polyoxometalate anions, this can become the rate-limiting step of the overall reaction when pathways such as reoxidation via H^+ or molecular O_2 are kinetically or thermodynamically unfavorable.[1i,5e,8a−c] According to the data obtained in this study, this limitation also holds for anion **1a**; e.g., complete oxidation of its reduced forms required 25−30 h (Figure 7) under the controlled conditions which imposed a slow rate of substrate conversion. A more rapid method for regeneration of the catalyst was sought by applying an electrode potential slightly more positive than that used in the first reversible redox process of the particular polyoxometalate anion.

To probe the feasibility of in situ electrolytic regeneration of a polyoxometalate catalyst, the photooxidation of BzOH in the presence of catalytic amounts of **1a** (6 mol %) was studied as a model system. A solution of **1a** (1.8 mM) and BzOH (30 mM) in MeCN (10 mL; supporting electrolyte $[Bu_4N]PF_6$, 0.05 mM) was irradiated with visible light (312−700 nm) at 23 °C in the electrolysis cell depicted in Figure 1. The experiment was conducted in three stages, with samples analyzed by gas chromatography and voltammetric measurements undertaken at various times. In the first stage, the reaction mixture was

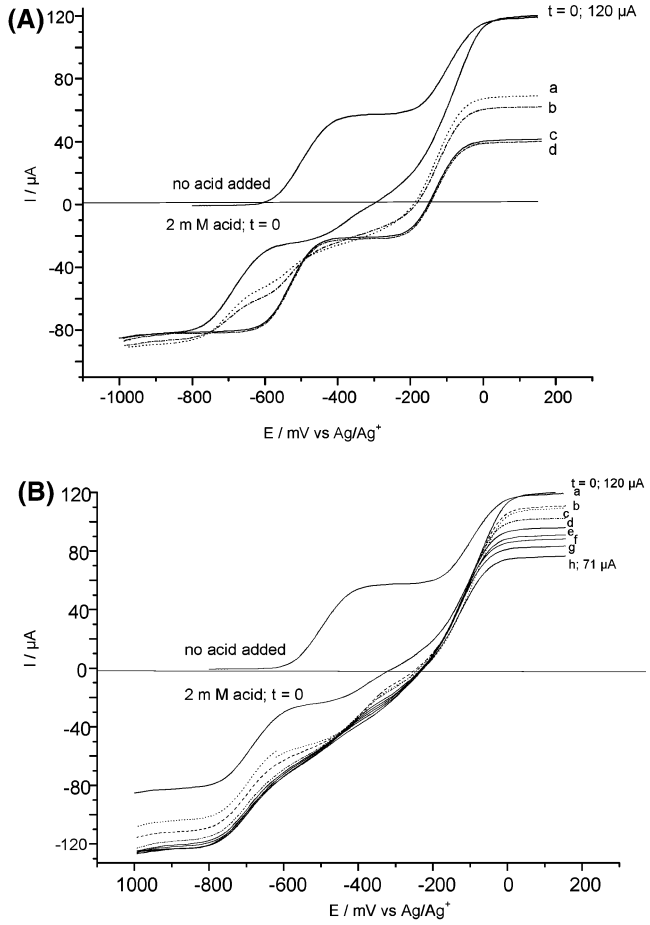

Figure 8. RDE voltammograms obtained at a GC electrode during the course of aerobic (A) and anaerobic (B) oxidation of $[S_2W_{18}O_{62}]^{6-}$ (2 mM) in the presence of 2 mM of CF_3SO_3H in MeCN 0.05 M Bu_4NPF_6). $\nu = 10$ mV s^{-1}, $N_r = 1000$ rpm. (A) t/I (min/μA) values: (a) 30/69.3, (b) 55/57.5, (c) 120/37, (d) 150/35. (B) t/I (min/μA) values: (a) 30/109, (b) 60/105, (c) 120/97, (d) 150/91, (e) 180/86, (f) 210/83, (g) 240/78, (h) 300/71.

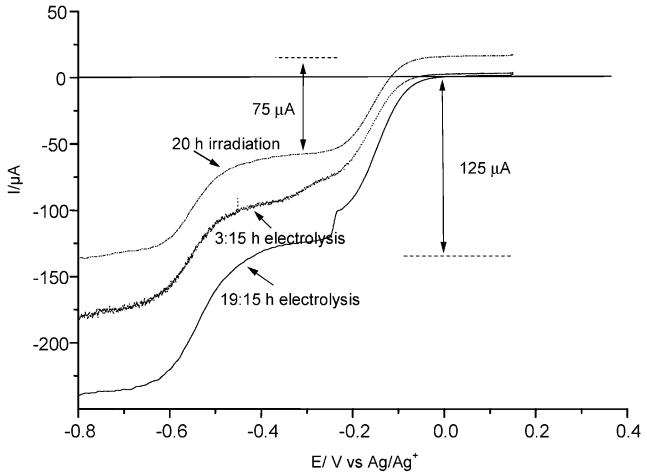

Figure 9. Dependence of RDE voltammograms obtained at a GC electrode during photolysis for 20 h followed by photolysis with in situ oxidative electrolysis to recover **1a**. Solution conditions: BzOH (30 mM) and **1a** (1.8 mM, 6 mol %) in 10 mL of MeCN (0.05 M Bu_4NPF_6). $\nu = 10$ mV s^{-1}, $N_r = 2500$ rpm.

irradiated without applying an external potential to the working electrode. As expected, a blue color developed, and oxidative currents detected voltammetrically indicated the generation of reduced forms of **1a** (Figure 9). In the second stage, the blue solution was subjected to controlled potential electrolysis (CPE) at +0.2 V (vs Ag/Ag^+) to achieve the oxidation of all reduced forms of the catalyst back to $[S_2W_{18}O_{62}]^{4-}$ (Table 1, Scheme 1). After complete oxidation of **1a**, the Pt gauze anode was replaced with a glassy carbon RDE, and irradiation of the solution continued. However, during this third stage of the experiment, the potential of the working electrode was continuously held at +0.2 V (CPE) and rotated at $N_r = 2500$ rpm. Over a period of 19 h, the solution remained almost colorless, consistent with the continuous presence of the oxidized form $[S_2W_{18}O_{62}]^{4-}$, whereas the oxidation of BzOH to benzaldehyde continued to occur. Consistent with the absence of a blue color, only negligible oxidative currents (≤ 2 μA) were detected in the RDE voltammograms (Figure 9). It was concluded that, under these conditions, rapid oxidation of the reduced species of **1a** formed in the photoreaction occurred at the surface of the rotating working electrode. Regenerated **1a** was swept back into the bulk solution, where it could again participate in the photoredox reaction. In this form of photoelectrochemical catalysis, regeneration of the catalyst is a simple electrochemical step, and protons generated in the photochemical step (eqs 1−4) are not expected to be consumed. In contrast, both the H^+ and O_2 pathways for catalyst regeneration lead to a decrease in $[H^+]$. The changes in the shapes, positions, and heights of the voltammetric waves when the catalyst is electrochemically regenerated are consistent with a steady increase in $[H^+]$ (compare Figures 5 and 9).

Photooxidation Reactions with $[Hex_4N]_4[S_2Mo_{18}O_{62}]$ (1b) and $[Bu_4N]_2[SMo_{12}O_{40}]$ (2). Protonation experiments were also undertaken with **1b** in neat MeCN solution. The two-electron-reduced **1b**($2e^-$) was generated in situ via CPE from **1b** (2 mM) in MeCN (0.1 M Bu_4NPF_6) and 4 mM of CF_3SO_3H added (Figure S4). Addition of acid leads to the characteristic behavior of **1b** and **1b**($2e^-$) observed in MeCN solution after addition of sufficient aqueous $HClO_4$.[9b] Thus, the first two initially well-resolved one-electron waves converted progressively into an overall two-electron wave, as did the second well-resolved pair of one-electron processes. Previous studies on the effect of protons on the voltammetry of **1b** in MeCN and in MeCN/H_2O (95:5), respectively, reported positive shifts in $E_{1/2}$ values of magnitudes similar to those found in this study ($\Delta E_{1/2} > 300$ mV).[9b,d]

The photooxidation of BzOH with catalytic amounts of **1b** was examined under conditions equivalent to those employed above for **1a**. In the absence of electrochemical regeneration, intense green/blue-colored solutions were observed, together with steady increases in the concentrations of benzaldehyde, protons, and reduced forms of **1b**. For this anion, neither the H^+ nor O_2 regeneration pathway is available, so the electrochemical approach remained as the only option available for the regeneration of the catalyst. As for **1a**, the catalyst could be regenerated by in situ electrolysis, and benzaldehyde continued to form while the reaction solution remained yellow/orange, indicative of the continuous presence of the oxidized form. The oxidation current detected in RDE measurements remained close to zero over time periods of up to 20 h. The electrochemical method therefore can be used to create catalytic pathways for polyoxometalate anions such as **1b** that are otherwise not suitable for catalytic processes involving catalyst regeneration with oxygen or hydrogen ions.

In addition, the photoactivity of the Keggin anion **2** was examined for the first time. This anion also exhibits reversible electrochemistry.[9c,12a,b] Oxidation of both EtOH and BzOH to the aldehydes was observed in acetone solution, with the rate varying linearly with light intensity. Our present work reveals that **2** also promotes the selective photooxidation of BzOH and EtOH into the respective aldehydes with generation of protons (eq 15).

$$RCH_2OH + [SMo_{12}O_{40}]^{2-} \rightarrow RCHO + [SM_{12}O_{40}]^{4-} + 2H^+ \quad (15)$$

It is clear from consideration of the results obtained from all of these experiments that the principle of in situ electrolytic regeneration of a reduced polyoxometalate catalyst will apply to a wide range of photooxidation reactions when the polyoxometalate redox processes are reversible.

Solvent-free reactions are environmentally attractive alternatives to those carried out in classic organic solvents. Although the quaternary cation salts examined here are insoluble in alcohols, aldehydes were detected after exposure of heterogeneous mixtures of liquid BzOH or EtOH and the polyoxometalate anions to artificial or diffuse natural daylight. The characteristic color change associated with the reduction of the polyoxometalate anions occurred (visual inspection) in the anions but not in the liquid phase.

Conclusions

The anions $[S_2W_{18}O_{62}]^{4-}$, $[S_2Mo_{18}O_{62}]^{4-}$, and $[S_2Mo_{12}O_{40}]^{2-}$ promote the photooxidation of organic substrates such as benzyl alcohol, ethanol, and (−)-menthol. Electrochemical methods, RDE voltammetry in particular, have proven to be valuable in monitoring the course of these photoredox reactions and confirm the presence of reduced forms of the anions and the formation of protons. Regeneration of the catalyst via oxidation by H^+ or

Scheme 2

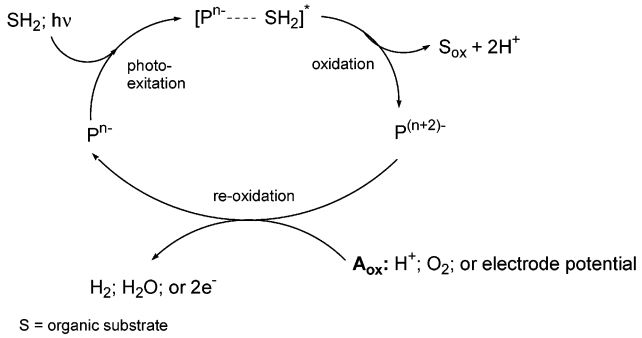

O_2 was possible for the $[S_2W_{18}O_{62}]^{4-}$ system, but not for $[S_2Mo_{18}O_{62}]^{4-}$ and $[SMo_{12}O_{40}]^{2-}$. However, in all cases a catalytic cycle may be achieved by conducting experiments in the presence of an electrode held at a potential that oxidizes the reduced polyoxometalates. On the basis of these studies, the photocatalytic cycle outlined in Scheme 2 can be written in a form which highlights the crucial oxidative regeneration step, which is needed to close the catalytic cycle.

The in situ electrochemical methods employed to study the outlined process provides information to establish the potential required for the regeneration of the reduced polyoxometalate catalyst. Thus, a photovoltaic cell or equivalent device can be used instead of a controlled potentiostat to generate the required external potential.

The slow rates of substrate conversions observed in the present study arise from the low intensity of the light source used (see Experimental Section) and long light path lengths. These reaction conditions permitted detailed electrochemical analysis of proton generation and consumption and of variation of redox and protonation states of the cluster anions. Conversions of BzOH of >50% can be achieved under the same conditions in less than 30 min when a 1000-W light source is used in combination with a mirror arrangement for the effective reflection of the light beam (see Experimental Section). This indicates that, when electrochemical regeneration of the catalyst is used (a rapid process), the light-dependent steps become rate determining. Synthetic applications will require efficient photochemistry via modified conditions including high-intensity light source, thin-layer cell, and efficient porous carbon channel electrode for catalyst regeneration.

Acknowledgment. The Australian Research Council is gratefully acknowledged for financial support of this project. We also thank Ronald Beckett, Water Studies Center, Monash University, for making a light source available to us.

Supporting Information Available: Figures S1 (voltammograms for the acid titration (CF_3SO_3H) of $[S_2W_{18}O_{62}]^{4-}$), S2 (oxidation of $[S_2W_{18}O_{62}]^{6-}/H^+$), S3 (voltammograms for the anaerobic oxidation of $[S_2W_{18}O_{62}]^{6-}$ in the presence of HBF_4), and S4 (voltammograms for the acid titration of $[S_2Mo_{18}O_{62}]^{6-}$) (PDF). This information is available free of charge via the Internet at http://pubs.acs.org.

JA029348F